Journal of Southeast University (English Edition) Vol.19 No.1 Mar. 2003 ISSN 1003—7985

Analysis of circular-to-circular groove waveguide junction

Cui Licheng Yang Hongsheng

(Department of Electronic Engineering, Southeast University, Nanjing 210096, China)
(State Key Laboratory of Millimeter Waves, Southeast University, Nanjing 210096, China)

Abstract: Mode matching method is used to analyze the scattering characteristics of the circular-to-circular groove waveguide junction. Matching the electric fields and magnetic fields at the boundary of the junction, and multiplying the mode functions of the circular waveguide and circular groove waveguide on both sides of the boundary equation, the scattering matrix equation is obtained, the scattering coefficients can be obtained from the equation. Then the scattering characteristics of the iris with circular window in circular groove waveguide are analyzed. At last the convergent problem is discussed; when choosing a suitable mode group, convergent numerical results are obtained, and the frequency response of the iris' scattering coefficients is also given.

Key words: circular groove waveguide; circular-to-circular groove waveguide junction; mode matching method

As a new type of transmission medium, circular groove waveguide has some attractive advantages, such as low loss, low dispersion, large dimension, and high power handling capacity, especially its large dimension. Circular groove waveguide can be used in millimeter and sub-millimeter waves[1].

As we know, the central region of the circular groove waveguide is a circular region, so it is easy for a circular groove waveguide to connect with a circular waveguide. In this case, the problem of circular-to-circular groove waveguide junction should be solved firstly. In this paper, a mode-matching method is used to deal with this problem.

Firstly modal functions of circular waveguide and circular groove waveguide are used to describe the electric and magnetic fields, then we match the transverse electric and magnetic field at the junction boundary. That leads to the scattering matrix equation. At last, the convergent problem of the numerical results is discussed; when a suitable mode group is chosen, convergent numerical results can be obtained.

1 Electric Field and Magnetic Field Mode Matching at the Junction

Fig.1 shows the structure of a circular-to-circular groove waveguide junction; the circular waveguide (waveguide 1) has a smaller dimension.

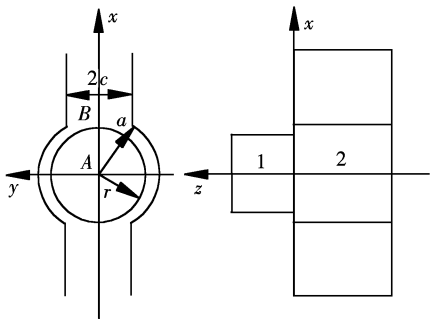

Fig.1 Circular-to-circular groove waveguide junction

In circular waveguide, the tangential electric field at $z = 0^+$ can be given as a superposition of transverse electric (TE) and transverse magnetic (TM) modal fields

$$\boldsymbol{e}_1(\rho,\alpha) = \sum_q \sum_s (a_{qs}^{(h)+} + a_{qs}^{(h)-})\boldsymbol{e}_{1,qs}^{(h)}(\rho,\alpha) + (a_{qs}^{(e)+} + a_{qs}^{(e)-})\boldsymbol{e}_{1,qs}^{(e)}(\rho,\alpha) \quad (1)$$

where $\boldsymbol{e}_{1,qs}^{(h)}(\rho,\alpha)$ and $\boldsymbol{e}_{1,qs}^{(e)}(\rho,\alpha)$ are TE and TM modal fields, respectively; $a_{qs}^{(h)+}$, $a_{qs}^{(h)-}$, $a_{qs}^{(e)+}$, $a_{qs}^{(e)-}$ are amplitude coefficients of $\boldsymbol{e}_{1,qs}^{(h)}(\rho,\alpha)$ and $\boldsymbol{e}_{1,qs}^{(e)}(\rho,\alpha)$, respectively; the superscripts + and − denote incident and scattering mode, respectively.

Assuming the incident wave is TE_{11} mode, then the modal fields in the circular waveguide can be expressed as[2]

$$\boldsymbol{e}_{1,qs}^{(h)}(\rho,\alpha) = N_{qs}^{(h)}\left[\frac{q}{\rho}J_q(\beta'_{qs}\rho)\cos q\alpha\,\hat{\rho} - \beta'_{qs}J'_q(\beta'_{qs}\rho)\sin q\alpha\,\hat{\alpha}\right] \quad (2)$$

Received 2002-10-30.
Biographies: Cui Licheng (1974—), male, graduate; Yang Hongsheng (corresponding author), male, professor, hsyang@seu.edu.cn.

$$\boldsymbol{e}_{1,qs}^{(e)}(\rho,\alpha) = N_{qs}^{(e)}\left[\beta''_{qs}J'_q(\beta''_{qs}\rho)\cos q\alpha\,\hat{\rho} - \frac{q}{\rho}J_q(\beta''_{qs}\rho)\sin q\alpha\,\hat{\alpha}\right] \tag{3}$$

where $q = 1,3,5\cdots$, $r = 1,2,3\cdots$; $N_{qs}^{(h)}$ and $N_{qs}^{(e)}$ are normalization constants; β'_{qs}, β''_{qs} are the s-th roots of $J'_q(x)$, $J''_q(x)$.

In circular groove waveguide, the tangential electric field at $z = 0^-$ can also be given as a superposition of TE and TM modal fields as

$$\boldsymbol{e}_2(x,y) = \sum_p\sum_l\sum_r (b_{plr}^{(h)+} + b_{plr}^{(h)-})\boldsymbol{e}_{2,plr}^{(h)}(x,y) + (b_{plr}^{(e)+} + b_{plr}^{(e)-})\boldsymbol{e}_{2,plr}^{(e)}(x,y) \tag{4}$$

where $\boldsymbol{e}_{2,plr}^{(h)}(x,y)$ and $\boldsymbol{e}_{2,plr}^{(e)}(x,y)$ are TE and TM modal fields, respectively; $b_{plr}^{(h)+}$ and $b_{plr}^{(h)-}$, $b_{plr}^{(e)+}$ and $b_{plr}^{(e)-}$ are amplitude coefficients of $\boldsymbol{e}_{2,plr}^{(h)}(x,y)$ and $\boldsymbol{e}_{2,plr}^{(e)}(x,y)$, respectively; superscripts + and − denote the incident and scattering modes, respectively.

Modal fields in circular groove waveguide have been discussed in detail in Ref. [1]. Here for clarity, we summarize the modal functions in a compact form as follows.

Region A

$$\boldsymbol{e}_{2,plr}^{(h)}(\rho,\alpha) = \sum_p H_p^{(h)}\left[\hat{\rho}\,\frac{p}{\rho}J_p(k_c^{(h)}\rho)\sin(p\alpha) - \hat{\alpha}k_c^{(h)}J'_p(k_c^{(h)}\rho)\cos(p\alpha)\right] \tag{5}$$

$$\boldsymbol{e}_{2,plr}^{(e)}(\rho,\alpha) = \sum_p H_p^{(e)}\left[\hat{\rho}k_c^{(e)}J'_p(k_c^{(e)}\rho)\sin(p\alpha) - \hat{\alpha}\,\frac{p}{\rho}J_p(k_c^{(e)}\rho)\cos(p\alpha)\right] \tag{6}$$

Region B

$$\boldsymbol{e}_{2,plr}^{(h)}(x,y) = \sum_r \hat{x}B_r^{(h)}k_{yr}^{(h)}\sin(k_{yr}^{(h)}y)\exp[-k_{xr}^{(h)}(x-x_0)] + \hat{y}B_r^{(h)}k_{xr}^{(h)}\cos(k_{yr}^{(h)}y)\exp[-k_{xr}^{(h)}(x-x_0)] \tag{7}$$

$$\boldsymbol{e}_{2,plr}^{(e)}(x,y) = \sum_r -\hat{x}B_r^{(e)}k_{xr}^{(e)}\sin(k_{yr}^{(e)}y)\exp[-k_{xr}^{(e)}(x-x_0)] - \hat{y}B_r^{(e)}k_{yr}^{(e)}\cos(k_{yr}^{(e)}y)\exp[-k_{xr}^{(e)}(x-x_0)] \tag{8}$$

where $p = 1,3,5\cdots$, $r = 1,3,5\cdots$; $H_p^{(i)}$ and $B_r^{(i)}(i = h,e)$ are the modal normalization factors of the circular groove waveguide; $k_c^{(i)}(i = h,e)$ is the cutoff wave number; $\mathrm{j}k_{xr}^{(i)}$ and $k_{yr}^{(i)}(i = h,e)$ are the wave numbers in x and y directions, respectively.

At the junction boundary, the electric field should be continuous in the circular aperture $0 \leqslant \rho \leqslant r$, and vanish everywhere else in the region of the circular groove waveguide cross section, so the boundary condition can be given as

$$\boldsymbol{e}_2(\rho,\alpha) = \begin{cases}\boldsymbol{e}_1(\rho,\alpha) & 0 \leqslant \rho \leqslant r\\ 0 & \text{elsewhere}\end{cases} \tag{9}$$

Substituting Eqs. (1) and (4) into Eq. (9), we get

$$\sum_p\sum_l\sum_r (b_{plr}^{(h)+} + b_{plr}^{(h)-})\boldsymbol{e}_{2,plr}^{(h)}(\rho,\alpha) + (b_{plr}^{(e)+} + b_{plr}^{(e)-})\boldsymbol{e}_{2,plr}^{(e)}(\rho,\alpha) = \begin{cases}\sum_q\sum_s (a_{qs}^{(h)+} + b_{qs}^{(h)-})\boldsymbol{e}_{1,qs}^{(h)}(\rho,\alpha) + (a_{qs}^{(e)+} + a_{qs}^{(e)-})\boldsymbol{e}_{1,qs}^{(e)}(\rho,\alpha) & 0 \leqslant \rho \leqslant r\\ 0 & \text{elsewhere}\end{cases} \tag{10}$$

Scalar multiplying $\boldsymbol{e}_{2,plr}^{(h)}(\rho,\alpha)$ on both sides of Eq. (10) and integrating over the complete cross section of circular groove waveguide, we obtain

$$b_{plr}^{(h)+} + b_{plr}^{(h)-} = \sum_q\sum_s H_{plr,qs}(a_{qs}^{(h)+} + a_{qs}^{(h)-}) + K_{plr,qs}(a_{qs}^{(e)+} + a_{qs}^{(e)-}) \tag{11}$$

where

$$H_{plr,qs} = \int_0^{2\pi}\int_0^r \boldsymbol{e}_{2,plr}^{(h)}(\rho,\alpha)\cdot\boldsymbol{e}_{1,qs}^{(h)}(\rho,\alpha)\rho\mathrm{d}\rho\mathrm{d}\alpha \tag{12}$$

$$K_{plr,qs} = \int_0^{2\pi}\int_0^r \boldsymbol{e}_{2,plr}^{(h)}(\rho,\alpha)\cdot\boldsymbol{e}_{1,qs}^{(e)}(\rho,\alpha)\rho\mathrm{d}\rho\mathrm{d}\alpha \tag{13}$$

Substituting the field functions into Eqs. (12) and (13), we obtain

$$H_{plr,qs} = \begin{cases}\int_0^r -H_p^{(h)}N_{ps}^{(h)}\pi[-k_c^{(h)}\rho J_{p+1}c\beta'_{qs}\rho J_{p+1}(\beta'_{ps}\rho) - 2p^2J_p(k_c^{(h)}\rho)J_p(\beta'_{ps}\rho) + \\ \qquad pJ_p(k_c^{(h)}\rho)J_p(\beta'_{ps}\rho) + k_c^{(h)}p\rho J_{p+1}(k_c^{(h)}\rho)J_{p1}(\beta'_{ps}\rho)]/\rho\mathrm{d}\rho & q = p\\ 0 & q \neq p\end{cases} \tag{14}$$

$$K_{plr,qs} = \begin{cases} \int_0^r -H_p^{(h)} N_{ps}^{(h)} p^2 \pi[-2J_p(k_c^{(h)}\rho)J_p(\beta''_{ps}\rho) + J_p(k_c^{(h)}\rho)J_{p+1}(\beta''_{ps}\rho)\beta''_{ps}\rho + \\ \qquad J_{p+1}(k_c^{(h)}\rho)J_p(\beta''_{ps}\rho)k_c^{(h)}\rho]/\rho \mathrm{d}\rho & q = p \\ 0 & q \neq p \end{cases} \tag{15}$$

Also scalar multiplying $\boldsymbol{e}_{2,plr}^{(e)}(\rho,\alpha)$ on both sides of Eq.(10) and integrating over the complete cross section of circular groove waveguide, we obtain

$$b_{plr}^{(e)+} + b_{plr}^{(e)-} = \sum_q \sum_s Q_{plr,qs}(a_{qs}^{(h)+} + a_{qs}^{(h)-}) + E_{plr,qs}(a_{qs}^{(e)+} + a_{qs}^{(e)-}) \tag{16}$$

where

$$Q_{plr,qs} = \int_0^{2\pi}\int_0^r \boldsymbol{e}_{2,plr}^{(e)}(\rho,\alpha) \cdot \boldsymbol{e}_{1,qs}^{(h)}(\rho,\alpha)\rho \mathrm{d}\rho \mathrm{d}\alpha \tag{17}$$

$$E_{plr,qs} = \int_0^{2\pi}\int_0^r \boldsymbol{e}_{2,plr}^{(e)}(\rho,\alpha) \cdot \boldsymbol{e}_{1,qs}^{(e)}(\rho,\alpha)\rho \mathrm{d}\rho \mathrm{d}\alpha \tag{18}$$

Substituting the field functions into Eqs.(17) and (18), we obtain

$$Q_{plr,qs} = \begin{cases} \int_0^r -H_p^{(e)} N_{ps}^{(h)} p^2 \pi[-2J_p(\beta'_{qs}\rho)J_p(k_c^{(e)}\rho) + J_{p+1}(k_c^{(e)}\rho)J_p(\beta'_{ps}\rho)k_c^{(e)}\rho + \\ \qquad J_p(k_c^{(e)}\rho)J_{p+1}(\beta'_{ps}\rho)\beta'_{ps}\rho]/\rho \mathrm{d}\rho & q = p \\ 0 & q \neq p \end{cases} \tag{19}$$

$$E_{plr,qs} = \begin{cases} \int_0^r H_p^{(e)} N_{ps}^{(e)} \pi[-pJ_p(k_c^{(e)}\rho)J_{p+1}(\beta''_{ps}\rho)\beta''_{ps}\rho - J_{p+1}(k_c^{(e)}\rho)J_p(\beta''_{ps}\rho) + \\ \qquad J_{p+1}(k_c^{(e)}\rho)k_c^{(e)}\rho J_{p+1}(\beta''_{ps}ps\rho)\beta''_{ps}\rho + 2p^2 J_{p+1}(k_c^{(e)}\rho)J_p(\beta''_{ps}\rho)]/\rho \mathrm{d}\rho & q = p \\ 0 & q \neq p \end{cases} \tag{20}$$

Eqs.(11) and (16) can be rewritten into matrix form

$$\boldsymbol{b} = \boldsymbol{M}\boldsymbol{a} \tag{21}$$

where

$$\boldsymbol{b} = \begin{Bmatrix} b^{(h)+} + b^{(h)-} \\ b^{(e)+} b^{(e)-} \end{Bmatrix}, \quad \boldsymbol{a} = \begin{Bmatrix} a^{(h)+} + a^{(h)-} \\ a^{(e)+} a^{(e)-} \end{Bmatrix}, \quad \boldsymbol{M} = \begin{bmatrix} \boldsymbol{H} & \boldsymbol{K} \\ \boldsymbol{Q} & \boldsymbol{E} \end{bmatrix}$$

For the magnetic field matching at the junction, the boundary condition is

$$\boldsymbol{h}_2(\rho,\alpha) = \boldsymbol{h}_1(\rho,\alpha) \qquad 0 \leqslant \rho \leqslant r \tag{22}$$

Using the same procedure as that of electric field matching, we can get[3]

$$\boldsymbol{M}^{\mathrm{T}}\boldsymbol{Y}_2(b^- - b^+) = \boldsymbol{Y}_1(a^- - a^+) \tag{23}$$

where

$$\boldsymbol{Y}_i = \begin{bmatrix} \boldsymbol{Y}_i^{(h)} & \boldsymbol{0} \\ \boldsymbol{0} & \boldsymbol{Y}_i^{(e)} \end{bmatrix} \qquad i = 1, 2$$

For the circular waveguide, the diagonal elements are

$$Y_{1,qs}^{(h)} = \frac{\sqrt{\beta'^2_{qs} - k_0^2}}{\mathrm{j}\omega\mu}, \quad Y_{1,qs}^{(e)} = \frac{\mathrm{j}\omega\varepsilon}{\sqrt{\beta''^2_{qs} - k_0^2}} \tag{24}$$

For the circular groove waveguide, the diagonal elements are

$$Y_{2,plr}^{(h)} = \frac{\sqrt{k_c^{(h)2} - k_0^2}}{\mathrm{j}\omega\mu}, \quad Y_{2,plr}^{(e)} = \frac{\mathrm{j}\omega\varepsilon}{\sqrt{k_c^{(e)2} - k_0^2}} \tag{25}$$

Solving Eqs.(21) and (23), we can get

$$\begin{Bmatrix} a^- \\ b^- \end{Bmatrix} = \begin{bmatrix} \boldsymbol{S}_{11} & \boldsymbol{S}_{12} \\ \boldsymbol{S}_{21} & \boldsymbol{S}_{22} \end{bmatrix} \begin{Bmatrix} a^+ \\ b^+ \end{Bmatrix} \tag{26}$$

where $\boldsymbol{S}_{11} = (\boldsymbol{Y}_1 + \boldsymbol{Y}_{L1})^{-1}(\boldsymbol{Y}_1 - \boldsymbol{Y}_{L1})$

$\boldsymbol{S}_{21} = \boldsymbol{M}(\boldsymbol{S}_{11} - \boldsymbol{I})$

$\boldsymbol{S}_{12} = 2(\boldsymbol{Y}_1 + \boldsymbol{Y}_{L1})^{-1}\boldsymbol{M}^{\mathrm{T}}\boldsymbol{Y}_2$

$\boldsymbol{S}_{22} = \boldsymbol{M}\boldsymbol{S}_{12} - \boldsymbol{I}$

$$\boldsymbol{Y}_{L1} = \boldsymbol{M}^{\mathrm{T}} \boldsymbol{Y}_2 \boldsymbol{M}$$

where $\boldsymbol{I}$ is the identity matrix.

2 The Iris with a Circular Window in the Circular Groove Waveguide

For the problem of the iris with a circular window in the circular groove waveguide, as shown in Fig.2, we can regard it as a cascading system, by using the results obtained in section 1, a generalized scattering matrix technique[3-7] can be applied to get the iris' scattering matrix.

3 Numerical Results

In the practical numerical calculation, the convergent problem should be considered carefully. It has been shown that the numerical results show a strong relationship to the chosen mode number[3,4,6]. Considering this, we choose four different mode groups, see Tab.1, and give their corresponding numerical results, see Fig.3. From the plot, we can see, when chosen 8 TE modes, 4 TM modes in circular waveguide, and 40 TE modes, 20 TM modes in the circular groove waveguide, the results have converged well. If there is no other explanation, this mode group will be chosen later.

Numerical results are also given for the iris with a circular window in a circular groove waveguide. The radius r of the iris is chosen as $\frac{1}{2}a$. Tab.2 gives the reflection coefficient Γ and transmission coefficient τ of the iris. It is easy to see that $|\Gamma|^2 + |\tau|^2$ almost equal 1. This fact also verifies the validity of the numerical results. Fig.4 gives the plot of reflection coefficient Γ and transmission coefficient τ with the variance of frequency.

Tab.1 Mode groups

Mode group	TE in circular waveguide	TM in circular waveguide	TE in circular groove waveguide	TM in circular groove waveguide
1	1	0	5	3
2	2	1	10	5
3	4	2	20	10
4	8	4	40	20

Tab.2 Some numerical results

Frequency/GHz	$\lvert\Gamma\rvert^2 + \lvert\tau\rvert^2$
85	0.999 235 439 899 06
86	0.999 577 843 023 29
87	0.999 238 532 761 93
88	0.999 227 779 859 86

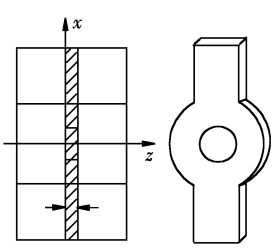

Fig.2 The iris with circular window in circular groove waveguide

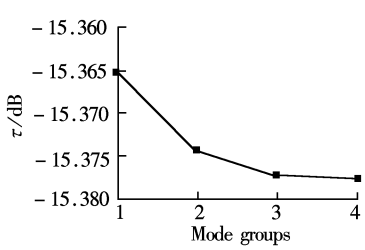

Fig.3 Variance of transmission coefficient τ of circular-to-circular groove waveguide junction with the change of mode group

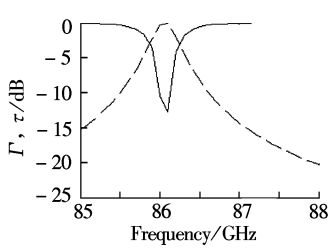

Fig.4 Γ and τ of the iris with the variance of frequency ($a = 2.85$ mm; $c = 1.85$ mm; $r = 1.43$ mm)

4 Conclusion

In this paper, mode-matching method is applied to analyze the scattering characteristics of a circular-to-circular groove waveguide junction. The convergent problem of the numerical results is discussed, along with the variance of scattering coefficients with the change of frequency. This job is a basic study, which can be widely used in designing filters, multiplexers, and oscillators.

References

[1] Yang H S, Ma J L, Lu Z Z. Circular groove guide for short millimeter and submillimeter waves [J]. *IEEE Trans Microwave Theory Tech*, 1995, **43**(2): 324-330.

[2] Collin R E. *Foundations for microwave engineering* [M]. New York: McGraw-Hill, 1966.

[3] Wade J D, MacPhie R H. Scattering at circular-to-rectangular waveguide junctions [J]. *IEEE Trans Microwave Theory Tech*, 1986, **34**

(11):1085 - 1091.

[4] Macphie R H, Wu K L. Scattering at the junction of a rectangular waveguide and a larger circular waveguide [J]. *IEEE Trans Microwave Theory Tech*, 1995, **43**(11): 2041 - 2045.

[5] Wu K L, Macphie R H. A rigorous analysis of a cross waveguide to large circular waveguide junction and its applications in waveguide filter design [J]. *IEEE Trans Microwave Theory Tech*, 1997, **45**(1): 153 - 157.

[6] Naini R S, Macphie R H. Scattering at rectangular-to-rectangular waveguide junctions [J]. *IEEE Trans Microwave Theory and Tech*, 1982, **30**(11): 2060 - 2063.

[7] Arndt F, Beyer R, Reiter J M, et al. Automated design of waveguide components using hybrid mode-matching/numerical EM building-blocks in optimization-oriented CAD frameworks-state of the art and recent advances [J]. *IEEE Trans Microwave Theory Tech*, 1997, **45**(5): 747 - 760.

圆-圆形槽波导结的研究

崔立成　　杨鸿生

(东南大学电子工程系,南京 210096)
(东南大学毫米波国家重点实验室,南京 210096)

摘　要　运用模式匹配法,分析了圆-圆形槽波导结的散射特性.在圆-圆形槽波导结上匹配电场和磁场的边界条件,然后在边界方程两边同乘以圆波导和圆形槽波导的模式方程,得到了散射矩阵方程,结的散射系数可由此方程得出.然后分析了圆形槽波导中放置圆形膜片的散射特性.最后讨论了数值计算结果的收敛性; 当选择恰当的模式组时,得到了收敛的数值结果,同时给出了膜片散射系数的频率响应结果.

关键词　圆形槽波导; 圆-圆形槽波导结; 模式匹配法

中图分类号　TN814